MADRID
inter.noise 2019
June 16 - 19
NOISE CONTROL FOR A BETTER ENVIRONMENT

Acoustic localization estimation of an Unmanned Aerial Vehicle using microphone array

Blanchard, Torea[1]

Thomas, Jean-Hugh[2]

Raoof, Kosai[3]

Laboratoire d'Acoustique de l'Université du Mans, LAUM UMR CNRS 6613
Avenue Olivier Messiaen, 72085 Le Mans, Cedex 9, France

Ecole Nationale Supérieure d'Ingénieurs du Mans, ENSIM
1 rue Aristote 72000 Le Mans, France

ABSTRACT

Acoustic source localization is an active research topic in array processing due to its multiple applications. Microphone array can be efficiently used for detecting, locating and tracking acoustic sources in their environment. In recent years, the current technological improvements of Unmanned Aerial Vehicles (UAV) have made drones more difficult to locate using optical or radio-based systems. However, the sound emitted by UAV motorization and their aerodynamic whistling can be exploited using a microphone array and an adequate real time signal processing algorithm. The purpose of this study is to characterize the acoustic signature of a drone and to estimate its 3D position using a microphone array with few sensors. Simple trajectories of the moving source are first simulated. Two methods, beamforming and goniometry, are tested to localize the source. Measurements were carried out in anechoïc conditions to characterize the acoustic signature of the drone. Additional measurements in real outdoor flight were finally made. Results obtained by the experiments are shown and the different approaches are compared to localize the drone and to track it. The performance in localization ability of the methods is studied.

Keywords: Acoustic localization, Beamforming, Goniometry
I-INCE Classification of Subject Number: 30

[1]torea.blanchard@univ-lemans.fr
[2]Jean-hugh.thomas@univ-lemans.fr
[3]kosai.raoof@univ-lemans.fr

1. INTRODUCTION

In recent years, the use of Unmanned Aerial Vehicles (UAVs) has become increasingly common since the technology to deploy them became widely easy. Moreover, the cost of drones is reduced with the technological improvements making them widely available in the market. Their applications are multiple. They can range from the simple hobbyist use (*e.g.* filmmaking) to business use as delivery services or for engineering firms using them mainly for maintenance inspections. Drones can also be used for environmental monitoring and conservation. However, in all cases, drones may show dangerous behaviour, whether voluntary or not. Indeed drones can easily fly near sensitive buildings or strategic airspaces such as ministries, airports or private spaces and show threatening behaviors. The current technological improvements of UAVs have made drones more difficult to locate using standard systems of surveillance such as radar or electro-optical systems. For these reasons, it has become critical to set up effective systems which are able to locate a drone flying over critical areas. The sound emitted by their motorization and their aerodynamic whistling can be exploited for the detection and localization tasks by using a microphone array.

Microphone arrays can be used efficiently to estimate the Direction of Arrival (DOA) of sources for several scenarios (*e.g.* indoor conditions showing high reverberation [1], outdoor conditions with UAV-embedded microphone array [2] or in submarine conditions [3]). Sound source localization techniques are divided into two main categories: Time-Direction-of-Arrival (TDOA) estimation methods and beamforming techniques. The first one is based on the cross-correlation function to estimate the time travelling of the acoustic wave emitted by the source between the pairwises of the microphone array. These methods can be viewed as a geometric approach as proposed by E. Van Lancker [4] or X. Alameda-Pineda and R. Horaud [5]. Beamforming techniques reconstruct the acoustic field using the signal recorded by the microphone array [6]. Signals recorded by the microphones are delayed in order to steer the antenna beam in a desired direction. Signal processing is then used to improve the ability of the array to separate close sources and improve its resolution.

Many researches have focused their effort on the localization of small UAV using acoustic measurements. For instance, E. E. Case et *al.* [7] designed a low-cost linear 24-microphones array to track the bearing angle of a small UAV using Time-Domain Delay-and-Sum Beamforming (TDDSB). However, the authors limited their localization for the 2D space case. An extended localization for the 3D space case was proposed by X. Chang et *al.* [8] using TDOA estimation algorithm based on the Generalized Cross-Correlation with Phase Transform (GCC-PHAT) function. They deployed two arrays of tetrahydron-shaped microphones to ensure localization in 3D space under the near-field hypothesis. Yet, the assumption of near-field is not always satisfied.

This paper presents a localization approach - under the far-field hypothesis, which limits the location to azimuth and elevation angles - applied to the tracking of a small commercial drone (Phantom IV advanced DJI) using a 3D-geometric 10-microphone array. Beamforming and acoustic goniometry are used for the localization task. The paper is organized as follows: Section 2 presents the theoretical background of the acoustic localization methods used, while Section 3 presents experimental measurements to evaluate the acoustic characteristics of a small UAV. Section 4 describes the experimental measurements which consist of locating the UAV using the microphone array designed for it. Results are presented and discussed.

2. ACOUSTIC LOCALIZATION METHODS

2.1. Time-Domain Delay-and-Sum Beamforming

The conventional Delay-and-Sum Beamforming (DSB) in time-domain can be processed in two main steps. First, each recorded acoustic pressure signal $p_m(t)$, where m refers to the m-th microphone, is shifted by a corresponding difference time $\tilde{\tau}_m(\Theta)$ depending on the focus direction Θ. In the far-field condition, the true delay τ_{nm} existing between the m-th and the n-th microphones can be determined from the distance between the microphones, the speed of sound c and the unitary vector $\mathbf{n}_s$ pointing the source direction Θ_s as

$$\tau_{nm}(\Theta_s) = c^{-1}(\mathbf{x}_m - \mathbf{x}_n)^T \mathbf{n}_s(\Theta_s), \tag{1}$$

where $\mathbf{x}_n$ indicates the vectorial position of the n-th microphone and ^{T} the transpose operator. The corresponding difference time $\tilde{\tau}_m(\Theta)$ is actually calculated according to a reference microphone. For an easier reading, the microphone indexed 0 is taken as the reference and placed at the origin of the referential so that $\mathbf{x}_0 = [0, 0, 0]^T$ and the subscript 0 is removed (*e.g.* $\tau_{0m} = \tau_m$). In this case, the delay applied at each microphone according to a desired direction is $\tilde{\tau}_m(\Theta) = c^{-1}\mathbf{x}_m^T\mathbf{n}_s(\Theta)$. The bearing and the elevation angles are defined such that the unitary vector pointing at the source is written $\mathbf{n}_s = [\cos\theta\cos\phi, \sin\theta\cos\phi, \sin\phi]^T$, where θ and ϕ are respectively the bearing and the elevation angles of the source. Finally, the signals are summed up and normalized by the number M of microphones giving one type of output beamforming signal:

$$p(t, \Theta) = \frac{1}{M}\left(p_{\text{ref}}(t) + \sum_{n=1}^{M-1} p_{\text{n}}(t + \tilde{\tau}_n(\Theta))\right). \tag{2}$$

$p_{\text{ref}}(t)$ is the acoustic pressure signal measured by the reference microphone. The source localization is ensured by the fact that the signals recorded by the microphones contain similar waveforms, but they are delayed. When the beamformer targets a true sound source position, *i.e.* $\Theta = \Theta_s$, the energy $|p|^2$ of the output beamforming signal is maximum. Signal components originating from other locations are neglected. Acoustic pressure signals are shifted according to a reference one to reconstruct the acoustic field surrounding the array.

2.2. Time-Frequency Delay-and-Sum Beamforming (TFDSB)

In TDDSB algorithm, the whole energy of the signals recorded is considered when calculating the beamforming output signal, which implies that the energy from undesirable frequencies is taken into account in the output signal. To overcome this limitation, each signal is filtered upstream the TDDSB stage to isolate the useful frequency bandwidth of the considered source signal. Thus, the energy of undesirable frequencies coming from other sources is attenuated and therefore the Signal-to-Noise Ratio (SNR) of the beamforming output signal is enhanced for the desired source signal. The frequency of the wanted source signal should be known. Moreover, the signal coming from other sources are supposed not to share the same frequency domain of emission with the desired source signal.

The method proposed in this study is to apply zero-phase shift bandpass filters on each signal to isolate only the harmonics wished. First the signals are frequency bandlimited

according to the frequency limits of the microphone array (see Section 2.3). The signal obtained is called Array Signal Framework. Harmonics having an amplitude higher than a fixed threshold in this bandwidth are then selected. For each selected harmonic, a zero-phase second-order bandpass filter with a quality factor $Q = 10$ is applied. The obtained signal is named Filtered Signal.

2.3. Frequency limit of the microphone array

The frequency bandwidth which is able, for a microphone array, to clearly locate acoustic sources is determined by some physical parameters depending on the array geometry and the sampling rate of the recordings. As well as the sampling rate restricts the spectral information of the signal according to the so-called Nyquist-Shannon sampling theorem, the upper limit frequency $f_{\max}$ of the array depends on the smallest distance d between two microphones as:

$$f_{\max} = \frac{c}{2d}. \tag{3}$$

Localization of narrowband source signal with frequency out of this limit may lead to spatial aliasing and the generation of pseudo-sources.

2.4. Acoustic goniometry

In the case of a far-field condition only, the DOA estimation of the source signal can be directly inferred from the TDOA estimation. For instance in the case of a signal impiging two microphones, spaced by d from an angle of θ, the TDOA τ is:

$$\tau = \frac{d}{c}\cos\theta, \tag{4}$$

where c is the speed of the sound in the air. In a three dimensional context, the DOA of a signal source is obtained by combining the TDOA estimation from multiple microphone pairs. In that case, the problem takes the following form :

$$\begin{gathered} \boldsymbol{\tau} = c^{-1}\mathbf{D}\mathbf{n}_s, \\ \boldsymbol{\tau} = [\ldots\ \tau_n\ \ldots]^T,\ \mathbf{D} = [\mathbf{x}_1\ \ldots\ \mathbf{x}_n\ \ldots\mathbf{x}_{M-1}]^T. \end{gathered} \tag{5}$$

where τ_n is the TDOA between the n-th microphone and the reference one, $\mathbf{x}_n$ is the vectorial position of the n-th microphone and $\mathbf{n}_s$ the normalized vector pointing the source position. $[.]^T$ indicates the transpose operator. To ensure a unique solution of Equation 5, $\mathbf{D}$ must be invertible which is the case if the antenna geometry is not plane. TDOA are estimated using GCC methods [10]. This approach is also known as acoustic goniometry due to its capability to give an angle estimation of an acoustic source.

3. ACOUSTIC CHARACTERIZATION OF A SMALL UAV

Acoustic characterization measurements were recorded on a small commercial UAV (Phantom IV advanced DJI). This measurement campaign aims (i) to identify the aerodynamic and the mechanical noises coming from the rotation of the propellers and the motors, (ii) to analyze the spectral variation of the signal emitted by the drone when a displacement direction is privileged and (iii) to determine the sound pressure level profile around the periphery of the drone in the propeller plane and underneath.

3.1. Material & measurement protocol

The acquisition system is constituted of a PXI-1036 Native Instrument device, a microphone BSWA Technology MPA 416 1/4" (20 Hz - 20 kHz) and a computer. Figure 1 shows the measurement scheme. Signals were recorded using SignalExpress 2015 software. A fast camera Phantom v5.1 was also used to measure the rotation frequency of the propellers. The measurements were made in the anechoïc chamber of the laboratory (with a low cutoff frequency of 70 Hz). The drone was fixed at 8 attachment points using nylon threads so that all measurements were made with the drone static. For the acoustic signature analysis of the drone, the microphone was placed in front of the drone in the propeller plane at a height of 80 cm. The microphone was placed at a distance of 150 cm from the drone. Each recording lasted 10 s with a sampling rate f_s of 30 kHz. The spectral estimation of the Power Spectral Density (PSD) was calculated using the Welch's method with Hanning windows of 10000 samples and 50% overlapping.

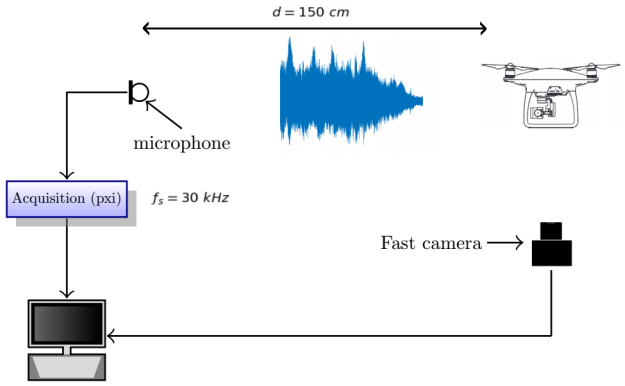

Figure 1: Scheme of the acoustic measurement for the analysis of the acoustic signature of the small UAV. A fast camera was used to measure the rotation speed of the propellers.

3.2. Results

3.2.1 Aerodynamic and mechanical sounds analysis

Measurements with and without propellers were carried out to analyze the contribution of the propellers and the motors to the total noise. The PSDs of the sound recorded with and without propellers for a fixed rotation speed are given in Figure 2. It can be observed that harmonics appear clearly up to 6 kHz when the propellers are mounted. The blade passing frequency have been estimated using the fast camera. The camera was calibrated to record 4000 images per seconds. The rotation frequency was therefore estimated to about 7742 tr.min^{-1}, *i.e.* 128 Hz. From this information, it can be deduced that the dominant tonal noise of the blade passing frequency is 256 Hz. Smaller harmonics can be observed at frequencies which are not multiple of the fundamental harmonic of the blade passing frequency. The acoustic behavior of the motor only is quite modified. The minor loading on the shaft of the motor may explain this change. The noise level of the motor covers mainly the mid range frequencies, *i.e.* between 1.5 kHz to 8 kHz. However, most part of the sound level when the propellers are mounted is still of aerodynamical origin.

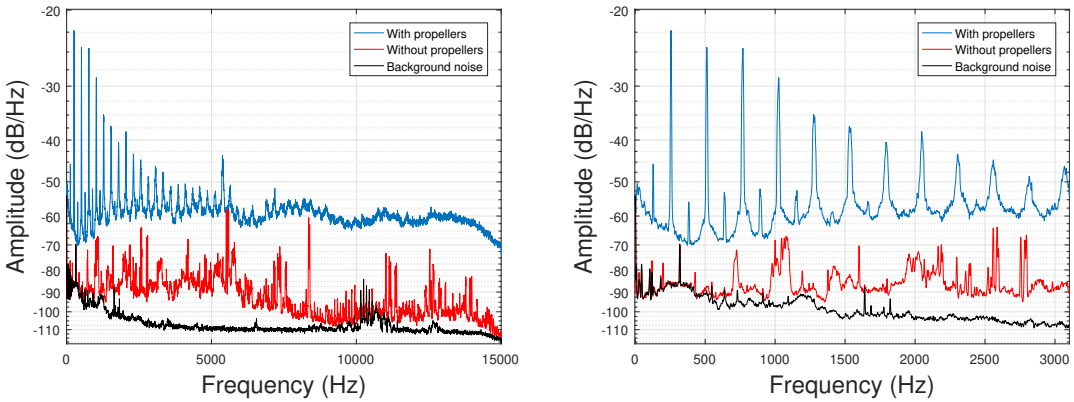

Figure 2: (left) Power Spectral Densities of the sound emitted by the drone with propellers (blue), without (red) and the background noise (black) of the anechoïc room and (right) a zoom up to 3 kHz.

3.2.2 Intermodulation analysis of the sound propellers

The influence of the sound emitted by the drone when the propellers have different blade passing frequencies was investigated. The drone displacement in the air is ensured by a differential thrust which exists between the individual thrusts from propellers. This difference induces a frequency shift of the harmonics of the signal as shown in Figure 3 where the PSD of the signal emitted by the drone when no direction is privileged is given in blue and the PSD of the signal when the controller imposes a displacement to the rigth in red. Measurements were made, one without a preferred direction and the others with different specific directions, at the same thrust. Low frequency harmonics (below 1 kHz) are slightly shifted - in the order of 5 to 10 Hz - while higher harmonics present more important shifting - in the order of a dozen hertz. Same results are obtained whatever the direction chosen.

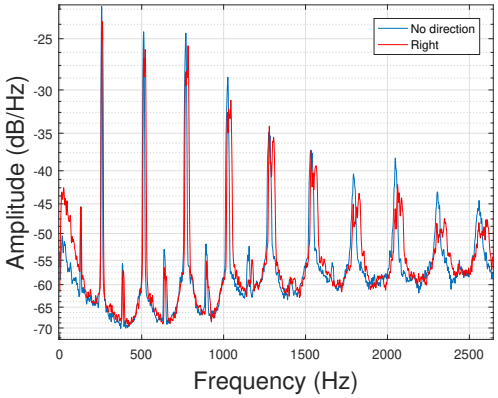

Figure 3: Power Spectral Densities of the sound emitted by the drone with propellers when no direction is privilegied (blue) and the right direction is imposed (red).

3.2.3 Peripherical and underneath sound pressure level measurement

The Sound Pressure Level (SPL) of the sound emitted around the periphery in the propeller-plane and underneath of the drone was measured. The sound pressure level P_{dB}

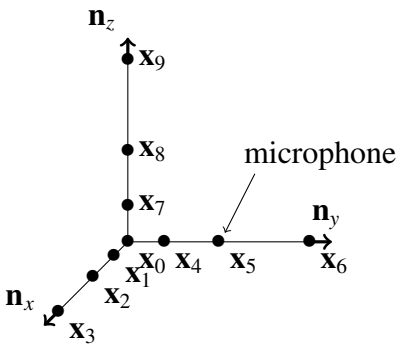

Figure 4: Scheme of the antenna geometry composed of ten microphones.

was estimated using the root mean square values of the signal x_{rms} and the noise b_{rms} as:

$$P_{\text{dB}} = 20 \log_{10} \left(\frac{x_{\text{rms}}}{b_{\text{rms}}} \right) \tag{6}$$

Results show that the SPL profile is omnidirectionnal in the periphery of the propeller-plane whereas it increases when it is measured underneath the drone. This results was expected due to the symmetry of the drone. The SPL is approximatively 94.5 dB in the propeller-plane and increases up to 97.5 dB when it goes underneath the drone at an angle of 34° from the propeller plane.

4. LOCALIZATION OF THE SMALL UAV

A 3D-geometric 10-microphone array (Figure 4) was designed to ensure the localization of the drone in both anechoïc and real conditions. The microphones were placed such that the upper frequency limit of the array is 2144 Hz for the anechoïc measurements and 3430 Hz in outside conditions. The speed of sound is fixed at $c = 343$ m.s^{-1}. The lower frequency of the bandpass filters for the TFDSB was fixed to 100 Hz. This bandwidth includes most of the harmonics of the sound emitted by the drone. The signals recorded by the microphones are split into 0.33 s and 0.5 s time segments for the TFDSB algorithm and the acoustic goniometry method respectively. The localization of the drone is then processed for each segment. The β-PHAT GCC function is used to estimate the TDOA with $\beta = 0.5$.

4.1. Anechoïc conditions

The drone was first placed in the ground at 3 m from the center of the antenna in the direction 45° in azimuth and 3.8° in elevation (the center of the drone was considered in the same plane as the propellers). The drone was flying vertically from the ground to a height of about 3.5 m with almost a constant speed (the drone was manually controlled). The position of the drone was estimated by a straight vertical trajectory at constant speed knowing the flight time and the departure and arrival positions. TFDSB location estimates were made for 4 different filtering operations and one without filtering. Each filtering allowed to select between 1 and 4 harmonics, ranging from fundamental to higher harmonics. The PSD of the reference microphone signal with 4 harmonics selected is given in Figure 5.

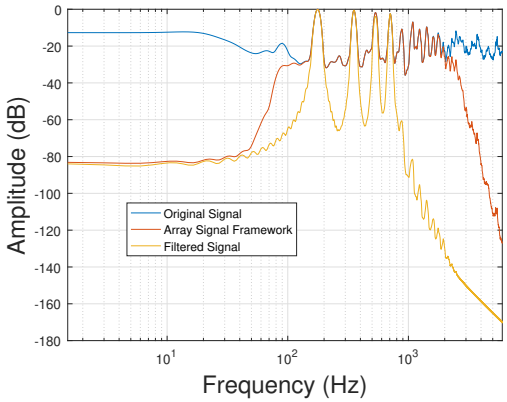

Figure 5: Power Spectral Densities of the original signal (blue), its array signal version (red) and its filtered version for the TFDSB (yellow) obtained from the reference microphone of the array in the anechoïc chamber. Four harmonics have been selected.

Location estimates of the drone for the TFDSB with 4 harmonics selected and the goniometry are given in Figure 6. According to the drone position measured before the flight and the estimation of the height reached, the elevation expected at its higher point is about 49.4°. The azimuth of the drone is still approximately the same during the flight. The acoustic goniometry method shows good results compared to those expected both in azimuth and elevation. However, inconsistent points at the begining and at the end of the flight (negative values of the elevation estimates) are present. This may be explained by the fact that the drone engines started and stopped respectively at that time (the drone is not flying), which could have led to false TDOA estimates. Nevertheless, errors are less than 10° in azimuth and elevation.

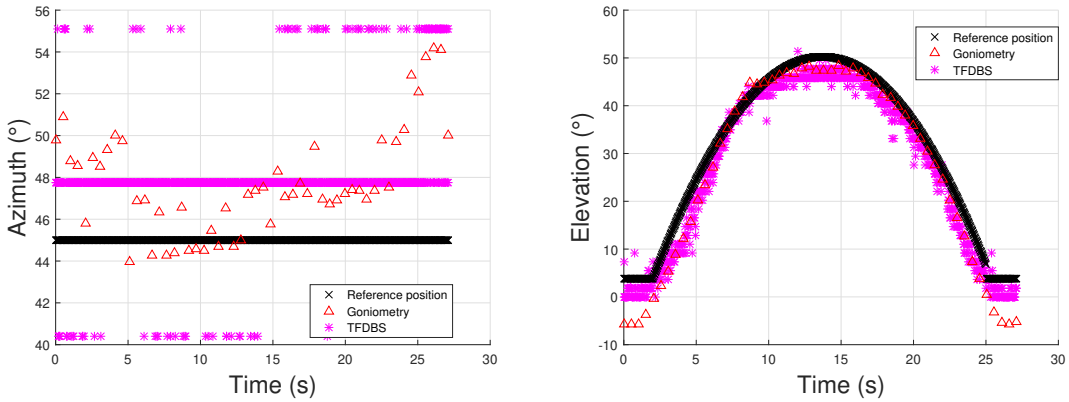

Figure 6: Results of the localization estimation of the drone using the TFDSB algorithm (magenta) and the acoustic goniometry method (red) for the anechoïc measurement conditions in azimuth (left) and elevation (right). Four harmonics have been selected.

The azimuth and elevation location errors for the TFDSB with multiple choices of filtering are given in Figure 7. The results show a slight deterioration in errors when the entire signal is taken into account. Noise from unwanted frequencies could affect the accuracy of location. In the other hand, location errors are more important if the number of harmonics selected is not sufficient.

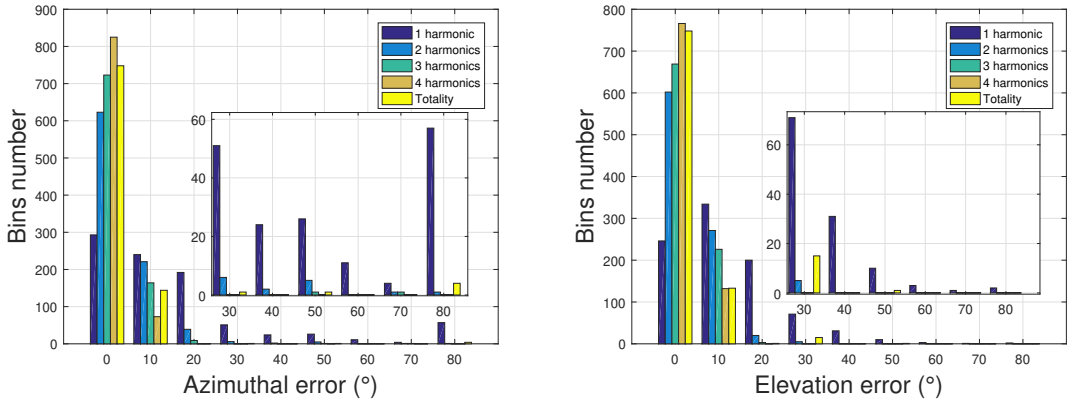

Figure 7: Histograms of drone location errors in the anechoïc chamber using TFDSB for different selected harmonics and the total signal in [0°, 80°] and by 10°-interval in azimuth (left) and elevation (right).

4.2. Outdoor measurements

Measurements in outdoor conditions were also made to compare the results with those obtained in the anechoic chamber. A similar trajectory was followed by the drone. The drone was placed at a distance of approximately 10.4 m and flew vertically at a height of approximately 5 m. The GPS coordinates of the array center were measured using the mobile's software. The cartesian x, y-coordinates of the drone are calculated using the latitude and longitude positions both of the drone, given its own GPS, and the array. The z-coordinate is given by the drone sensor. Finally, the cartesian coordinates are converted into spherical coordinates to obtain the azimuth and the elevation angles of the drone over the time.

Difficulties occured for the time synchronization of the data recorded by the microphone array and the drone timer. This may explain the slight time shift visible on the elevation plot in Figure 8. Moreover, the low precision (±8 m) of the array position from the GPS data (a difference of 8 m giving a deviation of approximately 37.5° at 10.4 m) should explain the difference between the estimates from localization algorithms and the GPS data. However, the methods allow to locate and follow the drone with a good fidelity compared to the original trajectory despite the presence of inconsistent points for the TFDSB algorithm at certain times.

Histograms of the errors in azimuth and elevation for the TFDSB with multiple choices of filtering are also given in Figure 9. Likewise the results in anechoïc condition, location estimates are better when harmonics are selected properly. Given the difficulties mentioned above, the errors are generally more significant. However, results in errors still better when the number of harmonics is sufficient (at least 2 in this case). The goniometry gives good results with errors less that 5° in elevation. The performance in azimuth is more difficult to evaluate due to the low GPS precision estimates.

"Realistic" trajectory measurements have also been made. The drone followed an arbitrary trajectory imposed by the controller. The trajectory followed by the drone is shown in Figure 10. The associated PSD of the signal recorded by the reference microphone is also provided.

The results obtained for the localization are shown in Figure 11. As mentioned above, there is a difference between the estimates of the azimuth of the drone based on acoustic measurements and GPS data due to the low accuracy of the GPS coordinates

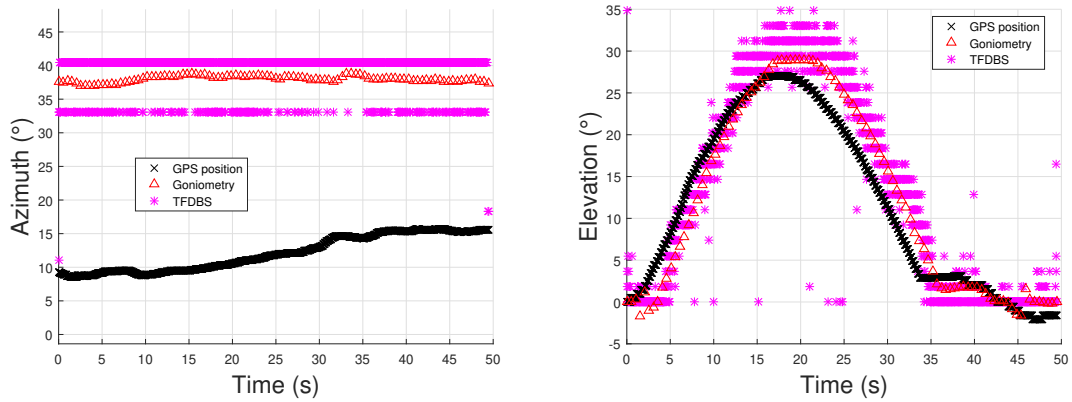

Figure 8: Results of the localization estimation of the drone using the TFDSB algorithm (magenta) with 4 harmonics selected and the acoustic goniometry method (red) for the outdoor measurement conditions in azimuth (left) and elevation (right).

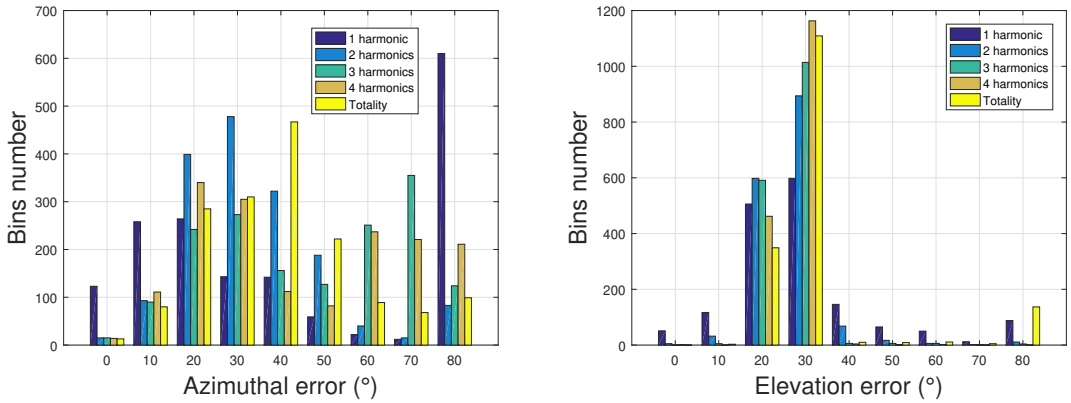

Figure 9: Histograms of drone location errors in outdoor using TFDSB for different selected harmonics and the total signal in [0°, 80°] and by 10°-interval in azimuth (left) and elevation (right).

provided by the mobile's software. Again, inconsistent points are present for estimates using the TFDSB algorithm. This is due to some higher energy in another direction when calculating the power of the beamforming output signal. Nevertheless, the TFDSB algorithm and the acoustic goniometry method make it possible to restore the overall trajectory followed by the drone during its flight.

5. CONCLUSION

The objectives of this study were to perform an acoustic analysis of a small commercial drone (DJI Phantom IV) in order to perform acoustic localization measurements. Two methods have been proposed to ensure the localization process. The first one is based on the so called Delay-&-Sum beamforming in the time domain. Preprocessing are used to isolate desired harmonics of the signals before the beamforming step. The second method is based on the estimation of the TDOA using the GCC function.

The acoustic characterization experiment of the drone consisted in (i) identifying the acoustic signature emitted by the drone with and without the propellers, (ii) evaluating the intermodulation of the sound emitted by the propellers and (iii) measuring the sound

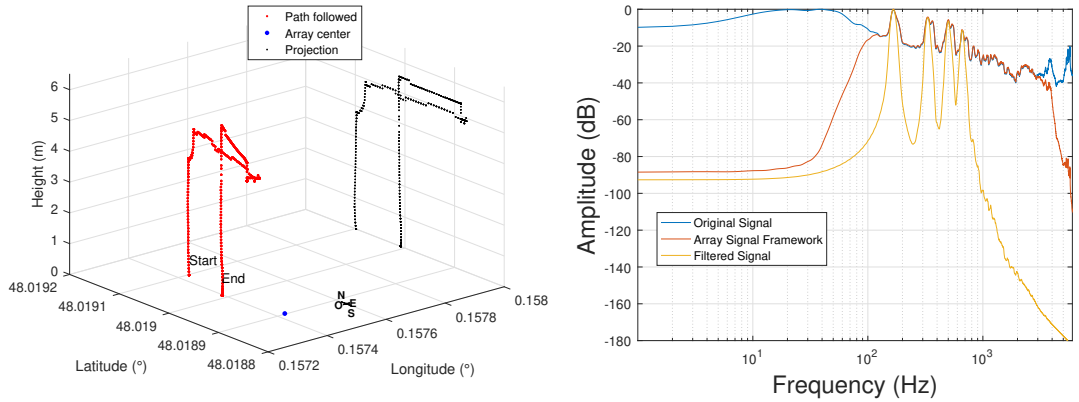

Figure 10: Trajectory followed by the drone for the "realistic" measurements (left) and the associated PSD of the reference signal for the TFDSB step (right) with 4 harmonics selected. The projection (black) allows to better estimate the height of the drone.

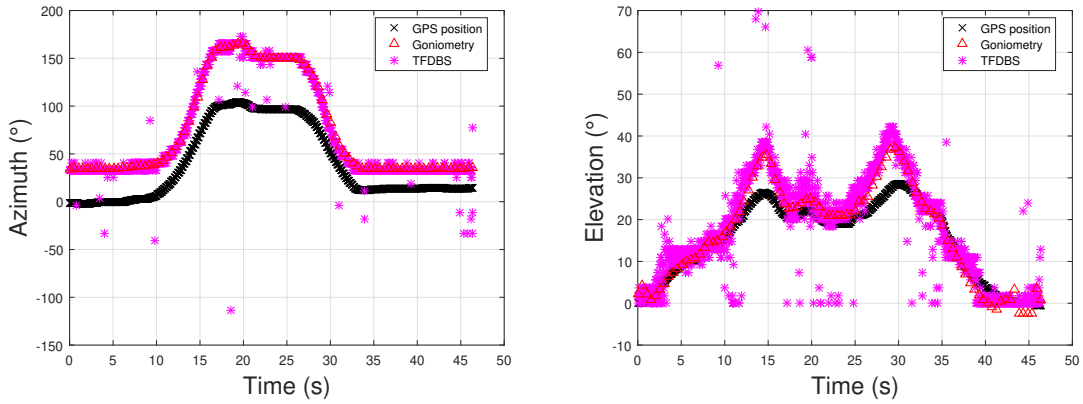

Figure 11: Results of the localization estimation of the drone using the TFDSB algorithm (magenta) with 4 harmonics selected and the acoustic goniometry method (red) for the outdoor measurement conditions in azimuth (left) and elevation (right).

level at the periphery and underneath the drone. The acoustic energy of the sound emitted by the drone is mainly of aerodynamic origin with harmonics of great amplitude at frequencies multiple of the double of the passage of a blade. The intermodulation of the different sounds from the propellers has been investigated. Low frequency harmonics are slightly shifted while high harmonics have more modulation. Finally, the peripheral and underneath sound pressure levels of the drone were measured. The SPL is invariant around the drone but the sound level is maximum (twice as much) at about 34° under the drone.

Experimental measurements were made in the anechoic chamber and outdoors. The microphone array was designed using data from acoustic characterization measurements. Some difficulties related to the temporal synchronization between the array data and the UAV data were encountered. The low accuracy of the GPS for the outdoor case did not allow to evaluate the actual performance of the results obtained by acoustic measurements. Nevertheless, the analysis of the data gives good results compared to those expected both in anechoic chamber and outside. In the case of the TFDSB algorithm, some estimates are inconsistent.

6. ACKNOWLEDGEMENTS

This work is funded by the Direction Générale de l'Armement (DGA).

7. REFERENCES

[1] Antigoni Tsiami, Athanasios Katsamanis, Petros Maragos, and Gerasimos Potamianos. Experiments in acoustic source localization using sparse arrays in adverse indoors environments. In *2014 22nd European Signal Processing Conference (EUSIPCO)*, pages 2390–2394. IEEE, 2014.

[2] Kotaro Hoshiba, Kai Washizaki, Mizuho Wakabayashi, Takahiro Ishiki, Makoto Kumon, Yoshiaki Bando, Daniel Gabriel, Kazuhiro Nakadai, and Hiroshi Okuno. Design of uav-embedded microphone array system for sound source localization in outdoor environments. *Sensors*, 17(11):2535, 2017.

[3] Juliana Lopez-Marulanda, Olivier Adam, Torea Blanchard, Marie Vallée, Dorian Cazau, and Fabienne Delfour. First results of an underwater 360° hd audio-video device for etho-acoustical studies on bottlenose dolphins (tursiops truncatus). *Aquatic Mammals*, 43(2), 2017.

[4] Eric Van Lancker. *Acoustic goniometry: a spatio-temporal approach*. PhD thesis, Verlag nicht ermittelbar, 2002.

[5] Xavier Alameda-Pineda and Radu Horaud. A geometric approach to sound source localization from time-delay estimates. *IEEE/ACM Transactions on Audio, Speech, and Language Processing*, 22(6):1082–1095, 2014.

[6] Barry D Van Veen and Kevin M Buckley. Beamforming: A versatile approach to spatial filtering. *IEEE assp magazine*, 5(2):4–24, 1988.

[7] Ellen E Case, Anne M Zelnio, and Brian D Rigling. Low-cost acoustic array for small uav detection and tracking. In *Aerospace and Electronics Conference, 2008. NAECON 2008. IEEE National*, pages 110–113. IEEE, 2008.

[8] Xianyu Chang, Chaoqun Yang, Junfeng Wu, Xiufang Shi, and Zhiguo Shi. A surveillance system for drone localization and tracking using acoustic arrays. In *2018 IEEE 10th Sensor Array and Multichannel Signal Processing Workshop (SAM)*, pages 573–577. IEEE, 2018.

[9] Jacek Dmochowski, Jacob Benesty, and Sofiène Affès. On spatial aliasing in microphone arrays. *IEEE Transactions on Signal Processing*, 57(4):1383–1395, 2009.

[10] Charles Knapp and Glifford Carter. The generalized correlation method for estimation of time delay. *IEEE transactions on acoustics, speech, and signal processing*, 24(4):320–327, 1976.